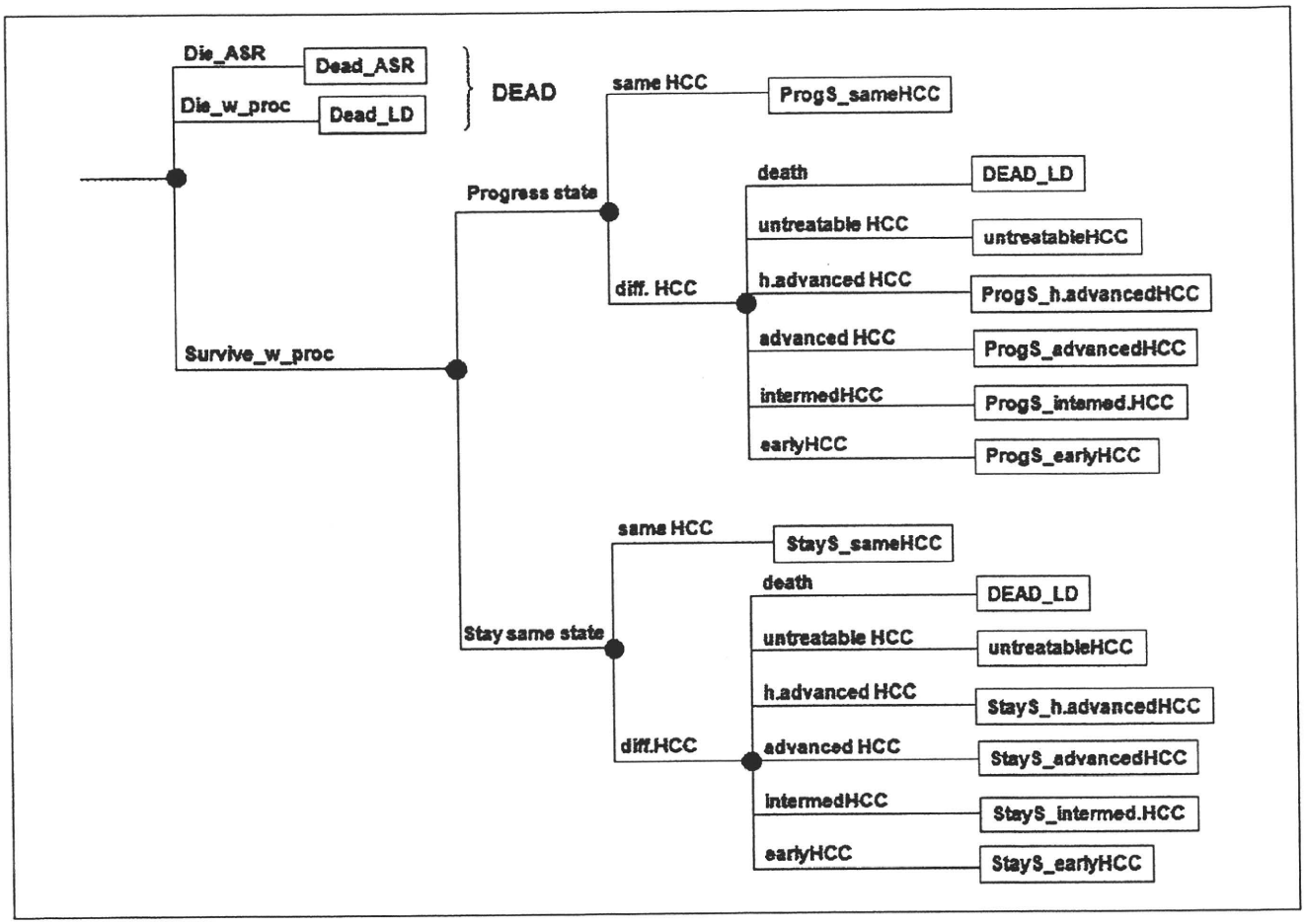

Fig. 4 Structure of sub-tree in one Markov cycle of our model. The first circular node, chance node, represents the probability of survival after therapeutic procedure ("survive_w_proc") and of death from age and sex ("die_ASR") or procedure-related death ("die_w_proc"). In the same cycle, underlying liver disease of survivors may progress from CH to compensated LC, or from compensated LC to decompensated LC ("progress state") or stay in the same condition ("same_state"). Patients may still remain in the same state of HCC after indicated therapeutic procedures ("same HCC"), or patients progressed to the advanced state or regressed to the improved one at the end of each cycle ("diff.HCC").

Simulation was performed on the TreeAge-Pro 2006 (TreeAge Software Inc.) with a one-month cycle and terminated when simulation reached 360 cycles (30 years) or the effectiveness of a cycle declined to be less than 0.001.

2.7 Validation of the Model

We validated the predictive performance of the model internally by comparing the survival curves using the actual data. As external validation, we also evaluated HR, LAT and TACE using the nationwide follow-up survey data. Cumulative survival rates were determined by patients registration data between 1992 and 2003 [8].

2.8 Statistical Analysis

The point estimation and 95% confidence intervals of the 1-year to 10-year survival rates were calculated using the Kaplan-Meier method and the Kalbfleisch and Prentice method [9]. The 95% CIs of survival curves predicted by the model were estimated by the simulation of a cohort with same size of the actual data without any censored cases.

3. Result

The monthly transition probability converted from the median transition period and the proportion of the next transitional states were basic data source of our model (Table 2). The median transition periods of initial treatment for early HCC states were 1859 days of HR and 1321 days of LAT, and those for non-early HCC were 484 days of LAT+TACE, 521 days of TACE and 508 days of HAIC, respectively. The corresponding periods of the treatment for recurrence were 460, 389, 390, 390, 297 days, respectively. The median transition period from one state to another in initial treatment declined progressively with the advance in the HCC state. The transition rates from initial treatment or recurrence one to progressed or regressed HCC states were also shown in Table 2. All of these figures were assigned in our Markov model.

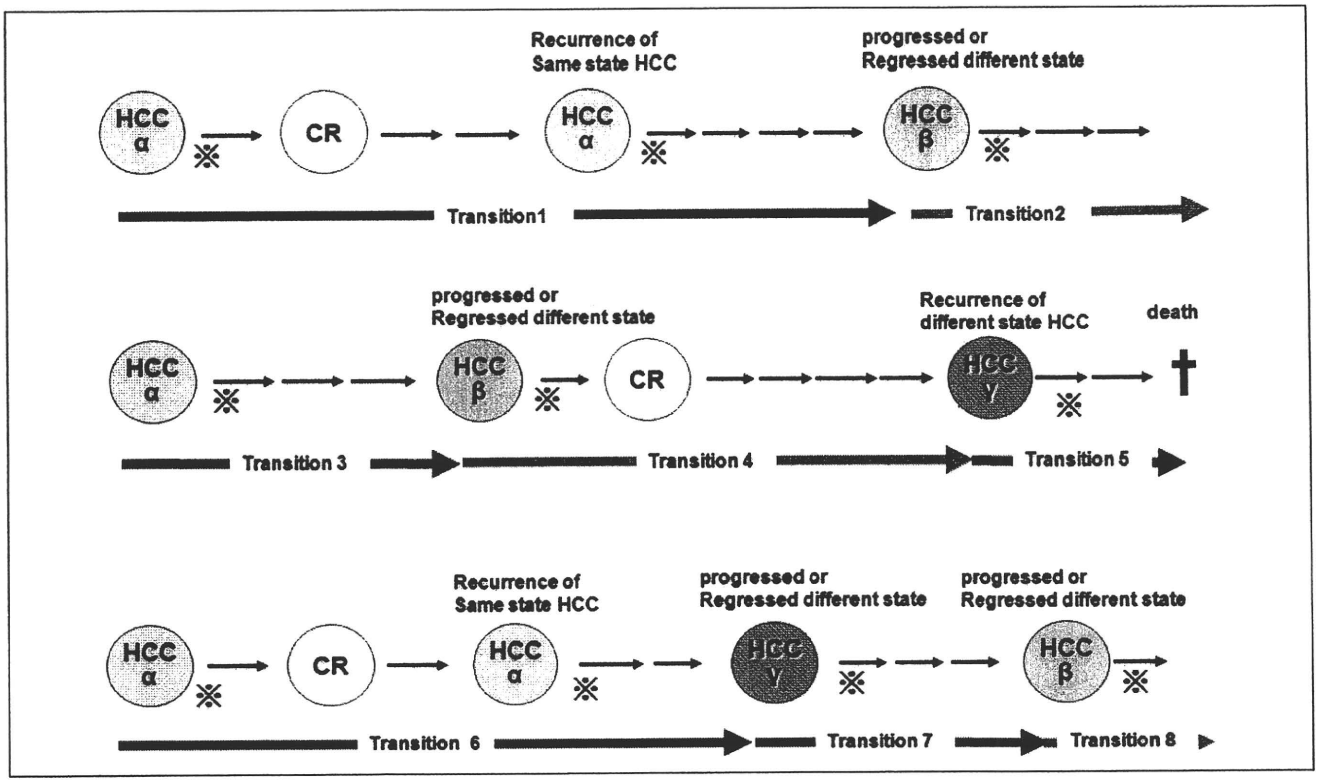

Fig. 5 Transition and length of transition period. Transition in our model was a change from one of the HCC states to the other irrespective of any treatment effect, such as complete remission or recurrence of the same state. The length of transition was obtained by the duration from the admission date for same HCC state to the admission date for different HCC state. For example, the transition periods for initial HCC α were estimated by the median periods of transition 1, 3 and 6 in the figure and two-thirds of the cases go to HCC β and one-third of the cases go to HCC γ. α, β and γ indicate the different HCC states, such as early, intermediate, advanced, etc. CR: complete remission. □ : treatment put into operation for each HCC state

Table 2 Transitional probabilities and the next transitional states

Stage	Treatment		Median (day)	Transitional probability (/month)	Next transitional state						
					Early		Intermediate	Advanced	Highly advanced	Terminal	Death
					HR	LAT					
Early HCC	HR	initial	1859	0.011	-	-	0.09	0.45	0.00	0.00	0.45
		recurrence	460	0.044	-	-	0.23	0.48	0.13	0.02	0.13
	LAT	initial	1321	0.016	-	-	0.32	0.37	0.22	0.02	0.18
		recurrence	389	0.052	-	-	0.30	0.42	0.10	0.06	0.12
Intermediate HCC	LAT+TACE	initial	484	0.042	0.03	0.20	-	0.60	0.06	0.04	0.07
		recurrence	390	0.052	0.04	0.19	-	0.57	0.09	0.01	0.10
Advanced HCC	TAC	initial	521	0.039	0.16	0.09	0.14	-	0.21	0.11	0.29
		recurrence	390	0.052	0.06	0.11	0.14	-	0.21	0.13	0.33
Highly advanced HCC	HAIC	initial	508	0.040	0.00	0.12	0.06	0.33	-	0.17	0.33
		recurrence	297	0.068	0.01	0.03	0.05	0.27	-	0.20	0.44
Terminal HCC			58	0.301	-	-	-	-	-	-	1.00

For internal validation, we compared the survival curves with 95% confidence interval (95% CI) bands between the Markov model and the KM method based on the original clinical data. Comparisons of their 1- to 10-year survival curve and rates of early HCC and non-early HCC were presented in Figures 6 and 7. These survival curves and the rates from the model for HR, LAT, TACE and HAIC exhibited substantial overlap within the 95% CIs. Representative 5-year survival comparisons between the KM curve and the Markov model were HR: 66% versus 60%, LAT: 74% versus 64%, LAT+TACE: 44% versus 38%, TACE: 34% vs. 31%, and HAIC: 24% vs. 26%, respectively. The difference between predicted survival rates and actual ones stayed within 10% in almost all treatment. The survival curves of HR were coarse and 95%CIs from the KM were fairly broad due to the small number of cases.

While the model may underestimate the survival for LAT+TACE (Fig. 7a), the survival curve was mostly sensitive to the transition probability of the initial treatment. If we adopt the transition rate at one year obtained from KM analysis of the cases, rather than the median transition period, to estimate the monthly transition probability after LAT+TACE treatment, it would be somewhat smaller (0.030) compared with the base data (0.042) and the predicted survival curve virtually overlapped the KM curve based on the actual data (Fig. 8).

On the other hand, predicted curves showed very analogous to those of external cohort. The predicted survival curve of HR by the Markov model overlapped with that for surveyed cases with solitary small (<2 cm in size) HCC with liver damage B as shown in Figure 9. Similarly, the survival curves of LAT by the Markov model overlapped with those of cases with solitary small HCC with liver damage A, and that the survival curve of TACE overlapped with HCC with liver damage A. These survival curves of the model and the nationwide survey were quite similar in their shapes (near linear decline in HR, sigmoidal decline in

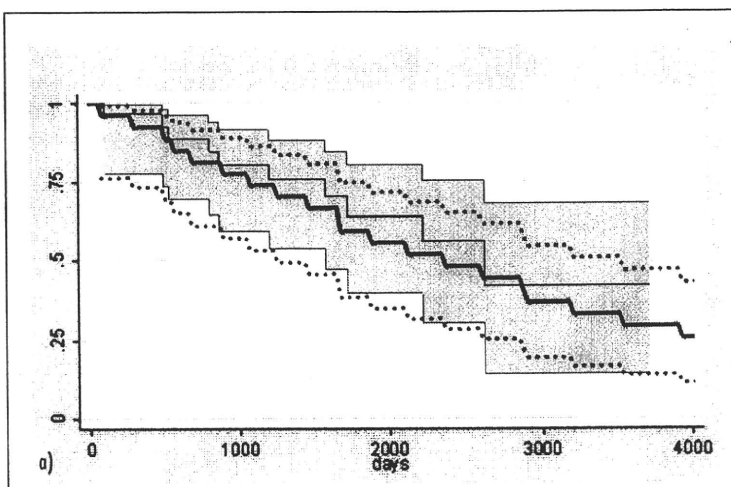

Year	Actual Data		Model	
	Survival	95%CI	Base	95%CI
1	1.00	.	0.92	(0.74-0.98)
2	0.92	(0.72-0.98)	0.84	(0.61-0.92)
3	0.83	(0.62-0.93)	0.76	(0.53-0.87)
4	0.79	(0.56-0.91)	0.68	(0.49-0.84)
5	0.66	(0.41-0.83)	0.60	(0.39-0.75)
6	0.66	(0.41-0.83)	0.53	(0.32-0.69)
7	0.58	(0.31-0.77)	0.47	(0.29-0.65)
8	0.44	(0.15-0.70)	0.41	(0.23-0.58)
9	0.44	(0.15-0.70)	0.35	(0.17-0.51)
10	0.44	(0.15-0.70)	0.31	(0.14-0.47)

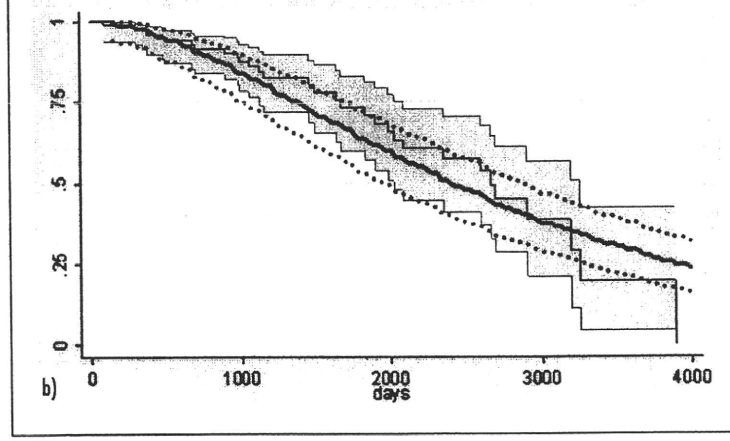

Year	Actual Data		Model	
	Survival	95%CI	Base	95%CI
1	0.98	(0.92-0.99)	0.96	(0.91-0.99)
2	0.92	(0.84-0.96)	0.90	(0.82-0.94)
3	0.86	(0.77-0.92)	0.81	(0.72-0.87)
4	0.83	(0.72-0.90)	0.73	(0.63-0.80)
5	0.74	(0.60-0.83)	0.64	(0.53-0.72)
6	0.61	(0.46-0.73)	0.55	(0.46-0.65)
7	0.58	(0.42-0.71)	0.47	(0.38-0.57)
8	0.39	(0.21-0.57)	0.40	(0.31-0.50)
9	0.20	(0.04-0.43)	0.34	(0.26-0.44)
10	0.20	(0.04-0.43)	0.29	(0.21-0.38)

Fig. 6 Survival curves of early HCC state (solitary and small tumor) predicted by the model and actual data. a) Initial treatment: hepatic resection; b) Initial treatment: LAT. The thick solid lines represent the predicted survival curves and dashed lines indicate their 95% confidence interval bands. The thin solid lines represent the KM survival curves from actual data and gray zones are their 95% confidence interval areas. The tables show the survival rates and their 95% confidence intervals at 1 to 10 years.

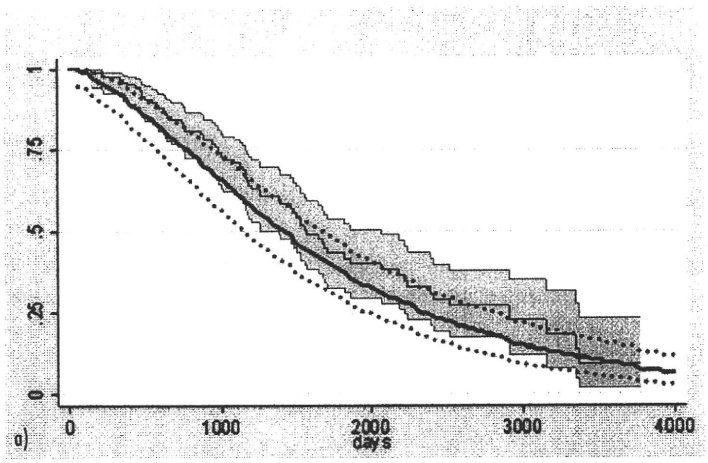

Year	Actual Data		Model	
	Survival	95%CI	Base	95%CI
1	0.96	(091-0.98)	0.91	(0.85-0.95)
2	0.84	(0.76-0.90)	0.77	(0.68-0.83)
3	0.71	(0.61-0.78)	0.62	(0.53-0.70)
4	0.58	(0.48-0.67)	0.49	(0.41-0.58)
5	0.44	(0.33-0.54)	0.38	(0.3-0.47)
6	0.37	(0.26-0.47)	0.30	(0.22-0.38)
7	0.27	(0.17-0.38)	0.22	(0.16-0.30)
8	0.23	(0.12-0.35)	0.17	(0.11-0.24)
9	0.18	(0.08-0.32)	0.13	(0.08-0.19)
10	0.09	(0.02-0.23)	0.09	(0.05-0.16)

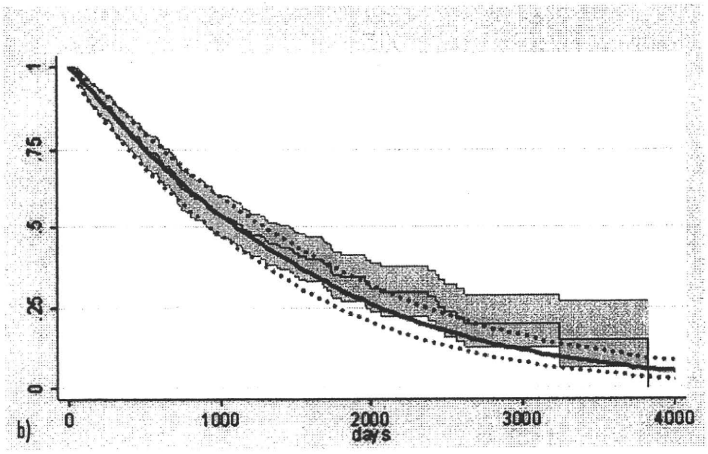

Year	Actual Data		Model	
	Survival	95%CI	Base	95%CI
1	0.82	(0.77-0.86)	0.82	(0.76-0.86)
2	0.64	(0.57-0.69)	0.65	(0.59-0.71)
3	0.52	(0.45-0.58)	0.51	(0.45-0.58)
4	0.44	(0.36-0.50)	0.40	(0.34-0.46)
5	0.34	(0.27-0.41)	0.31	(0.25-0.36)
6	0.30	(0.22-0.37)	0.23	(0.18-0.29)
7	0.24	(0.16-0.32)	0.18	(0.13-0.23)
8	0.20	(0.13-0.29)	0.13	(0.09-0.18)
9	0.15	(0.06-0.27)	0.10	(0.07-0.14)
10	0.15	(0.06-0.27)	0.07	(0.05-0.11)

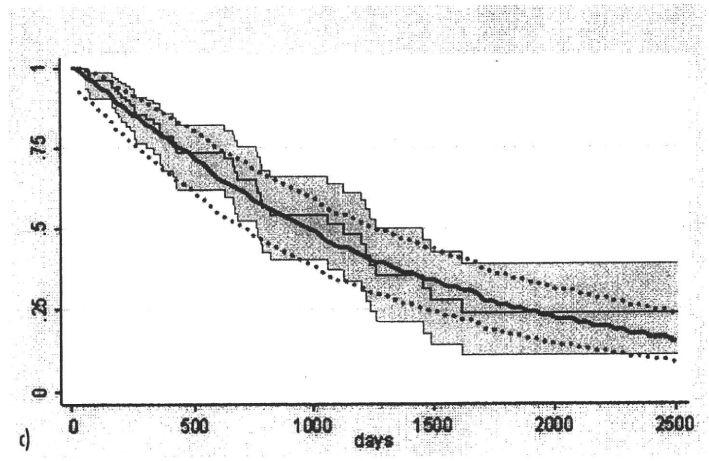

Year	Actual Data		Model	
	Survival	95%CI	Base	95%CI
1	0.80	(0.70-0.87)	0.79	(0.69-0.86)
2	0.65	(0.52-0.75)	0.60	(0.50-0.70)
3	0.51	(0.37-0.64)	0.46	(0.34-0.55)
4	0.32	(0.17-0.47)	0.35	(0.25-0.45)
5	0.24	(0.11-0.39)	0.26	(0.17-0.35)
6	0.24	(0.11-0.39)	0.19	(0.12-0.28)

Fig. 7 Survival curves of non-early HCC states predicted by the model and actual data. a) Initial treatment: combination of LAT and TACE; b) initial treatment: TACE; c) initial treatment: HAIC and systemic chemotherapy

LAT and exponential decline in TACE) supporting the external validity of the Markov model.

4. Discussion

Great progress in the diagnosis and treatment for HCC over several decades brought improvement of its prognosis, however, the optimal management of HCC remains controversial. The reason is that the uncertainty to estimate prognosis by pretreatment factors including tumor characteristics [10] and high recurrence rate make it difficult to predict prognosis after various treatment procedures.

Our Markov model which assumed the treatment procedures as health states and incorporated two phase of transition probabilities predicted prognosis of various stage of HCC accurately. There have been several reports of Markov models predicting the natural course of HCC in studies for the cost-effectiveness of surveillance or therapy for HCC [11-16]. However, they had several different points compared with our model. Firstly, their models used single transitional probability after different treatment for HCC led to monotonous decline of the survival. As far as we surveyed using MEDLINE, all simulation models to estimate the prognosis after interventions for HCC had applied single transition probabilities in the whole course [11, 13, 16, 17]. Secondly, they used many variables obtained from several published studies which were different in study design and sample characteristics. Therefore, their variables incorporated in their models consisted of heterogeneous ones. Thirdly, the validations of models were insufficiently in almost all reports, and it was difficult to justify the appropriateness of their results.

On the contrary, our model using the Markov process had the following characteristics. Firstly, it was constructed based on hypothetical HCC states expressed by the concordant treatments and liver fibrotic states. We assumed the initial treatment would be selected by tumor characteristics and preserved liver function according to the treatment strategy of Yamaguchi University Hospital which was comparable to those of the Japanese clinical practice guidelines for HCC [18].

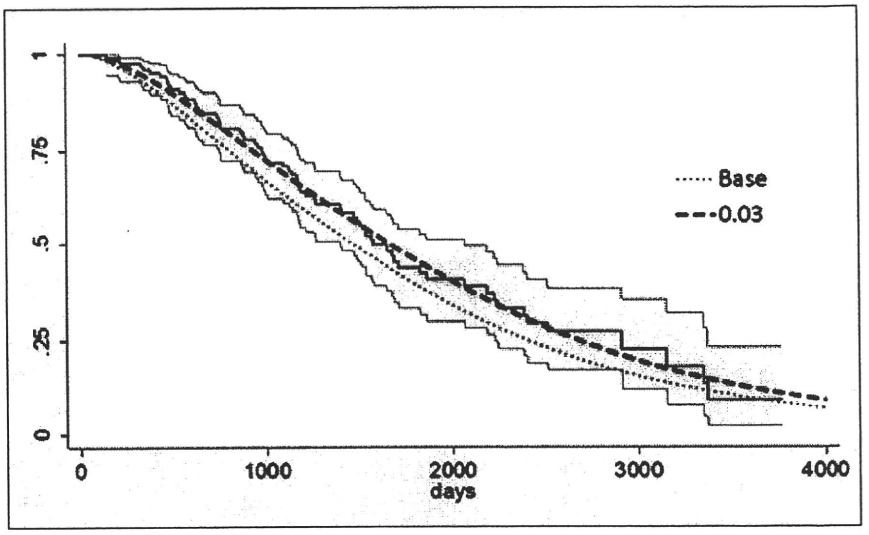

Fig. 8 Survival curves after adjustment of the transition probability from the initial LAT+TACE treatment. Dashed lines indicate the predicted survival curves and the solid line indicates the KM survival curves from actual data with gray zones representing the 95% confidence interval area.

Secondly, it used two-phase transition probabilities. It enabled us to evaluate the effect of the initial treatment correctly and project over a life-long course by recurrence. Frequent recurrences are common in HCV-related HCC and the effect of treatment tends to decline along with the recurrences. Moreover, the effect of initial treatments were found to be significantly and independently associated with patient survival as well as tumor characteristics. Those were determinant at the initial treatment [19]. Therefore, we grouped the model into the initial treatment state and the succeeding states for recurrences. Due to this separation, differences between the estimated transition periods from the initial treatment and those from treatments for recurrence in each HCC state was disclosed and more precise prediction of the prognosis could be expected.

Mathematical models have been proposed to predict prognosis, including the stochastic survival model using Cox regression model [20, 21], the hidden Markov [22] and the ordinary Markov model [23], and the discrete-event model [24]. Moreover, recent advances in computing have made it feasible to deal with more complicated methods that require time-consuming calculations, such as Bayesian estimation with Markov Chain Monte Carlo [25]. Among these models that can be applied to the clinical decision support, the Markov model has been characterized by its simplicity of model structure, its convenience in calculating the prognosis, and its responsible representation of many kinds of clinical problems [26]. Markov models are particularly useful in solving clinical problems that involve continuous risks that are ongoing over time. They are also useful for problems with repetitive events occurring with uncertain timing, which are difficult to deal with by a simple tree model. Modeling by conventional decision tree may require unrealistic or unjustified simplifying assumptions [27]. There is evidently trade-off in the relationship between the simplicity of the model and close reflection of the clinical course. The simpler the model structure is, the fewer the parameters in the model and the easier to understand, but the more risk of overestimation or underestimation. However, our Markov model enabled to allow incorporate the different treatment for the different stage of recurrence and hepatologists could accept the model because of its closeness to the clinical reality.

The predicted survival curves by the model were all consistent with the actual

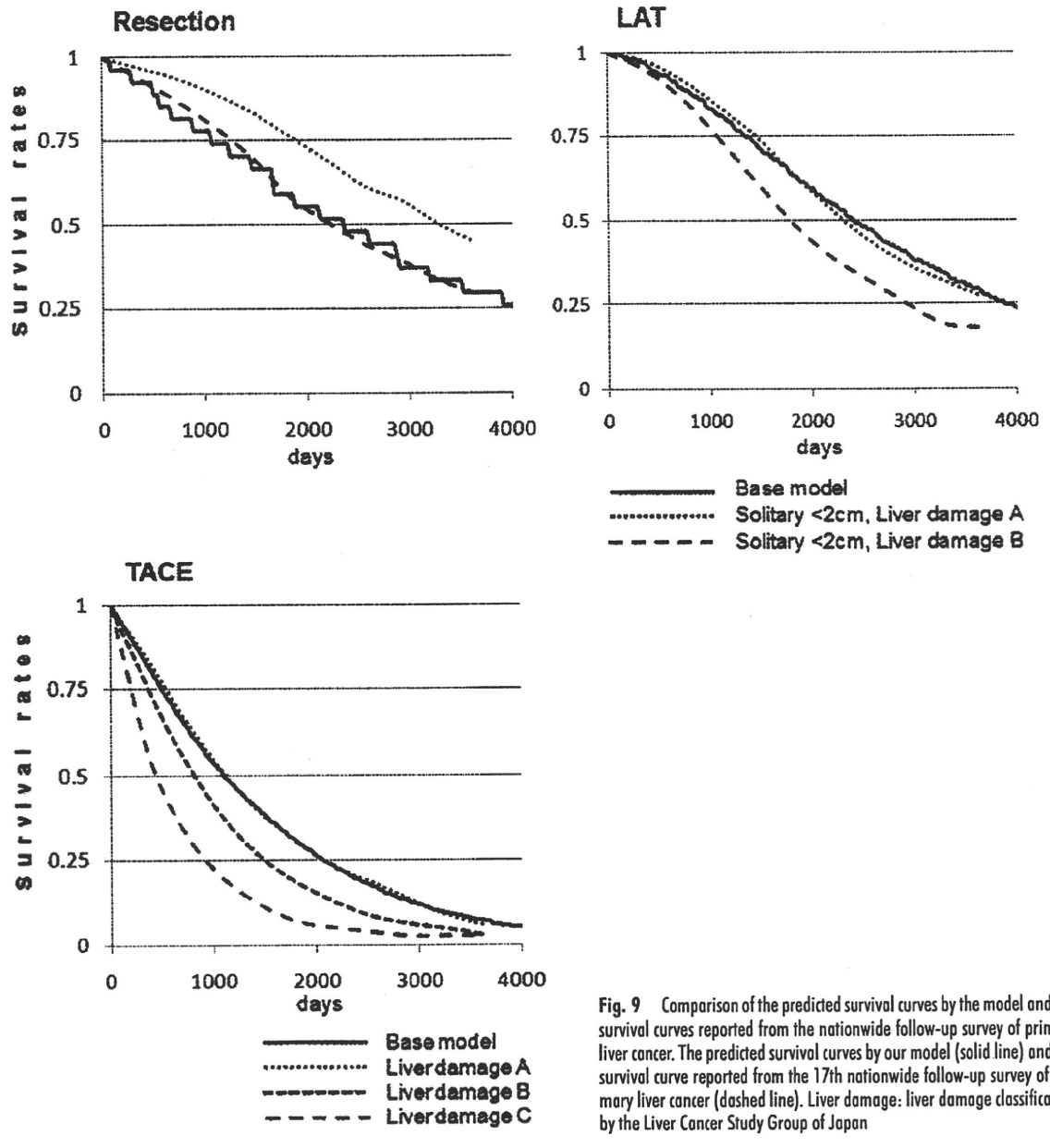

Fig. 9 Comparison of the predicted survival curves by the model and the survival curves reported from the nationwide follow-up survey of primary liver cancer. The predicted survival curves by our model (solid line) and the survival curve reported from the 17th nationwide follow-up survey of primary liver cancer (dashed line). Liver damage: liver damage classification by the Liver Cancer Study Group of Japan

curves except for LAT + TACE. The indication of this combination therapy was for oligo-nodular HCC, that is single segmental or sub-segmental lesion and distant small focal lesion. We considered these HCC states to be as intermediate states between the early HCC state and advanced one that optimal initial treatment was TACE. However, 60% of HCC cases treated by LAT + TACE as the initial treatment were treated by TACE at the next different state. It was possible that a proportion of this group might have originally been the same HCC states, which ought to be treated by TACE. Moreover, sensitivity analysis showed that the predicted curves were mostly affected by the initial transition probabilities. The estimated transition probabilities varied with the methods although we selected the median transition period for base case analysis rather than the person-year method, mean transition period or transition rate at a certain period. If the transition probability from the initial LAT + TACE was set at 0.03, which was obtained from the transition rate at one year from KM, and converted to the monthly probability, the predicted survival curve virtually overlapped with the KM curve based on the actual data. This result,

therefore, indicated that estimation of the initial transition probabilities was crucial and we needed to know which method was best to accurately obtain figures of transition state. Considering time-dependent variables could be the limitation of simple Markov model

Comparing the predicted survival curves by model and those of the external survey data for HR, LAT and TACE, the shape of these curves were quite similar; although those from our actual data were superior to those of the external one.

Our model has the following limitations: Firstly, the model does not consider liver transplantation, while the number of living-donor liver transplantations (LDLT) from patients' relatives has increased in Japan [28]. Unfortunately, we had few cases of liver-transplantation, the criteria of liver-transplantation appear to be expanding and consensus has not been established. However, LDLT has increased worldwide and the successful results have been reported even in Japan [29]. Thus, we should incorporate the health state of liver transplantation in further trials if we can obtain sufficient data [30, 31].

Secondly, the cause of liver disease-related death included decompensated liver cirrhosis without HCC and terminal HCC state. The decompensated liver condition without HCC was considered as a consequent state after treatment for HCC and they frequently coexist. It is difficult to discriminate which is the direct cause, we did not distinguish between them.

Thirdly, we used retrospective data from three university hospitals, and combined them in one group. There were some differences in the prognosis among these facilities, especially HAIC. There might be some differences in selection criterion which affected sensitively on the estimation of survival curve. The prognosis after an initial treatment may be influenced by such criteria. Therefore, when we apply this model to cost-effectiveness and comparing the treatment, we need to adjust for the demographic factor, the HCC and the preserved liver state of the cases.

5. Conclusion

We constructed a Markov model that consisted of the first (initial) and the succeeding different treatment state. The survival curves from the model were close to those of the actual data, except for in the case of combination therapy with LAT and TACE, and were quite similar to those of external data.

Both internal and external validity of the developed Markov model for prediction of the prognosis after initial treatment for various HCC states were verified using actual and nation-wide survey data. The Markov model should be considered suitable for estimating the cost-effectiveness of screening and treatments for HCC.

Acknowledgment
This study was supported by the grant of Ministry of Health and Welfare (No. 204) in Japan and the Grant-in-Aid for Scientific Research from the Ministry of Education, Culture, Sports, Science and Technology of Japan (No. 20390152).

References

1. Okita K. Clinical aspects of hepatocellular carcinoma in Japan. Intern Med 2006; 45 (5): 229-233.
2. Llovet JM, Fuster J, Bruix J. The Barcelona approach: diagnosis, staging, and treatment of hepatocellular carcinoma. Liver Transpl 2004; 10 (2 Suppl 1): S115-20.
3. Llovet JM, Burroughs A, Bruix J. Hepatocellular carcinoma. Lancet 2003; 362 (9399): 1907-1917.
4. Rougier P, Mitry E, Barbare JC, Taieb J. Hepatocellular carcinoma (HCC): an update. Semin Oncol 2007; 34 (2 Suppl 1): S12-20.
5. Beck JR, Kassirer JP, Pauker SG. A convenient approximation of life expectancy (the "DEALE"). I. Validation of the method. Am J Med 1982; 73 (6): 883-888.
6. Beck JR, Pauker SG, Gottlieb JE, Klein K, Kassirer JP. A convenient approximation of life expectancy (the "DEALE"). II. Use in medical decision-making. Am J Med 1982; 73 (6): 889-897.
7. Ishida H, Inoue Y, Kurokawa F, Hino K, Okita K. Cost-effectiveness of screening program for Hepatitis C virus related hepatocellular carcinoma. Japan Journal of Medical Informatics 2002; 27 (suppl): 139-140.
8. Ikai I, Arii S, Okazaki M, Okita K, Omata M, Kojiro M, et al. Report of the 17th Nationwide Follow-up Survey of Primary Liver Cancer in Japan. Hepatol Res 2007; 37 (9): 676-691.
9. Kalbfleisch JD, Prentice RL. The Statistical Analysis of Failure Time Data. 2nd ed. New York: Wiley-Interscience; 2002.
10. Martins A, Cortez-Pinto H, Marques-Vidal P, Mendes N, Silva S, Fatela N, et al. Treatment and prognostic factors in patients with hepatocellular carcinoma. Liver Int 2006; 26 (6): 680-687.
11. Arguedas MR, Chen VK, Eloubeidi MA, Fallon MB. Screening for hepatocellular carcinoma in patients with hepatitis C cirrhosis: a cost-utility analysis. Am J Gastroenterol 2003; 98 (3): 679-690.
12. Hoshida Y, Shiratori Y, Omata M. Cost-effectiveness of adjuvant interferon therapy after surgical resection of Hepatitis C-related hepatocellular carcinoma. Liver 2002; 22 (6): 479-485.
13. Lin OS, Keeffe EB, Sanders GD, Owens DK. Cost-effectiveness of screening for hepatocellular carcinoma in patients with cirrhosis due to chronic hepatitis C. Aliment Pharmacol Ther 2004; 19 (11): 1159-1172.
14. Patel D, Terrault NA, Yao FY, Bass NM, Ladabaum U. Cost-effectiveness of hepatocellular carcinoma surveillance in patients with hepatitis C virus-related cirrhosis. Clin Gastroenterol Hepatol 2005; 3 (1): 75-84.
15. Saab S, Ly D, Nieto J, Kanwal F, Lu D, Raman S, et al. Hepatocellular carcinoma screening in patients waiting for liver transplantation: a decision analytic model. Liver Transpl 2003; 9 (7): 672-681.
16. Sarasin FP, Giostra E, Hadengue A. Cost-effectiveness of screening for detection of small hepatocellular carcinoma in western patients with Child-Pugh class A cirrhosis. Am J Med 1996; 101 (4): 422-434.
17. Nouso K, Tanaka H, Uematsu S, Shiraga K, Okamoto R, Onishi H, et al. Cost-effectiveness of the surveillance program of hepatocellular carcinoma depends on the medical circumstances. J Gastroenterol Hepatol 2008; 23 (3): 437-444.
18. Group formed to establish "Guidelines for evidence-based clinical practice for the treatment of liver cancer". Clinical practice guidelines for hepatocellular carcinoma. Tokyo: Kanehara & Co., Ltd.; 2005.
19. Toyoda H, Kumada T, Kiriyama S, Sone Y, Tanikawa M, Hisanaga Y, et al. Changes in the characteristics and survival rate of hepatocellular carcinoma from 1976 to 2000: analysis of 1365 patients in a single institution in Japan. Cancer 2004; 100 (11): 2415-2421.
20. Chevret S, Leporrier M, Chastang C. Measures of treatment effectiveness on tumour response and survival: a multi-state model approach. Stat Med 2000; 19 (6): 837-848.
21. Keiding N, Klein JP, Horowitz MM. Multi-state models and outcome prediction in bone marrow transplantation. Stat Med 2001; 20 (12): 1871-1885.
22. Wallis RS. Mathematical modeling of the cause of tuberculosis during tumor necrosis factor blockade. Arthritis Rheum 2008; 58 (4): 947-952.
23. Faddy MJ, McClean SI. Markov chain modelling for geriatric patient care. Methods Inf Med 2005; 44 (3): 369-373.
24. Smolen HJ, Cohen DJ, Samsa GP, Toole JF, Klein RW, Furiak NM, et al. Development, validation, and application of a microsimulation model to

predict stroke and mortality in medically managed asymptomatic patients with significant carotid artery stenosis. Value Health 2007; 10 (6): 489-497.
25. Vanness DJ, Kim WR. Bayesian estimation, simulation and uncertainty analysis: the cost-effectiveness of ganciclovir prophylaxis in liver transplantation. Health Econ 2002; 11 (6): 551-566.
26. Beck JR, Pauker SG. The Markov process in medical prognosis. Med Decis Making 1983; 3 (4): 419-458.
27. Sonnenberg FA, Beck JR. Markov models in medical decision making: a practical guide. Med Decis Making 1993; 13 (4): 322-238.
28. Makuuchi M, Sano K. The surgical approach to HCC: our progress and results in Japan. Liver Transpl 2004; 10 (2 Suppl 1): S46-52.
29. Sugawara Y, Makuuchi M. Living donor liver transplantation: present status and recent advances. Br Med Bull 2005; 75-76: 15-28.
30. Llovet JM, Schwartz M, Fuster J, Bruix J. Expanded criteria for hepatocellular carcinoma through down-staging prior to liver transplantation: not yet there. Semin Liver Dis 2006; 26 (3): 248-253.
31. Onaca N, Davis GL, Goldstein RM, Jennings LW, Klintmalm GB. Expanded criteria for liver transplantation in patients with hepatocellular carcinoma: a report from the International Registry of Hepatic Tumors in Liver Transplantation. Liver Transpl 2007;13 (3): 391-399.

Correspondence to:
Haku Ishida, M.D.
1-1-1 Minami-kogushi Ube
Yamaguchi 755-8505
Japan
E-Mail: hishida@yamaguchi-u.ac.jp

肝胆膵　第57巻第6号　2008年(平成20年)12月28日発行(毎月1回28日発行)昭和56年2月3日第3種郵便物認可 ISSN 0389-4991　KAN-TAI

KAN・TAN・SUI (Japan)

肝胆膵

2008 12

特集●肝胆膵疾患とQOL

Vol.57 No.6 Dec. 2008　アークメディア

肝癌の病名告知と長期管理

吉岡奈穂子* 富山恭行* 日野啓輔*

索引用語：C型肝炎，インターフェロン，栄養療法，特殊アミノ酸製剤

1 はじめに

わが国の肝細胞癌のほとんどがウイルス性慢性肝疾患患者に発症し，肝炎ウイルスの持続感染による炎症と肝線維化は肝発癌と密接な関係にあることが報告されている．肝細胞癌発生の高危険群の設定により，わが国の肝細胞癌は早期に発見されることが多く，それ故生存率が向上し長期管理が必要となる．本稿では肝細胞癌の長期管理には病名告知が不可欠であること，そしてQOLを保ちながら長期生存を目指すにはどのような長期管理が必要かについて解説する．

2 肝癌の病名告知

肝細胞癌患者に対する検査や治療のInformed Consent（IC）を得るためには癌の告知をすることが前提となる．わが国では肝細胞癌のほとんどが肝炎ウイルス持続感染者に発症することが知られ，患者においても肝炎ウイルスが発癌ウイルスであることを知る者は多い．肝細胞癌の長期管理には血管造影や経皮的局所療法などの侵襲的検査や治療が不可欠であり，患者との信頼関係を構築するためにも積極的な肝癌の病名告知が必要となる．その一方で癌の告知を希望する患者も増加している．肝細胞癌では慢性肝炎の時期から長期間にわたり同じ患者に接する機会が多く，患者の病名告知に対する考えや死生観について知り得ることが可能な場合がある．この点は他の癌と比べると病名告知が行いやすい点かもしれない．

肝細胞癌の告知は原則として本人に伝え，家族にも患者と共に話を聞いてもらう．がん告知後に患者と家族におこる精神的反応[1]を理解し，看護師，精神科医，臨床心理士などのスタッフとチームで診療にあたるべきである．肝細胞癌は治療を行っても再発を繰り返すことが多いため，まず「肝細胞癌は5年以内に80％が再発する」といわれるほど非常に再発率が高いことを患者に伝えるべきである．しかし，この場合もいたずらに再発率の高さを強調して患者の不安を煽ることは厳に慎むべきであり，長期にわたる治療に協力し

Naoko YOSHIOKA et al: Informed consent and long-term management in patients with hepatocellular carcinoma
*川崎医科大学附属病院肝胆膵内科［〒701–0192 倉敷市松島 577］

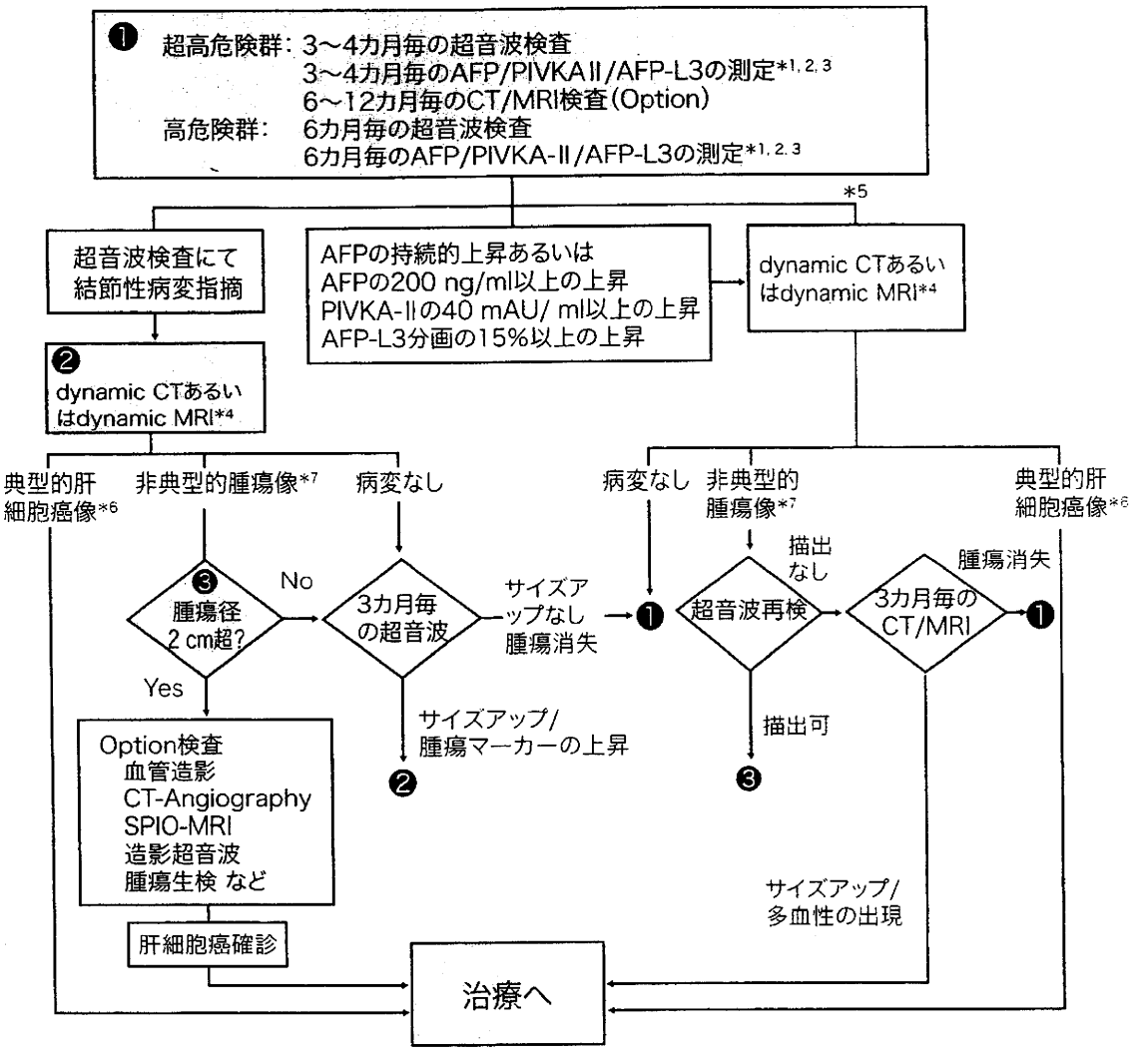

図1　肝細胞癌サーベイランスのアルゴリズム

＊1　現行の健康保険では，腫瘍マーカーは，毎月1種類しか測定できない．

＊2　AFP-L3分画は，肝細胞癌の病名がついていないと測定できない．

＊3　AFPが10 ng/ml以下の場合，AFP-L3分画は測定できない．

＊4　腎機能障害がある場合，ヨード造影剤アレルギーが疑われる場合，dynamic MRIが推奨される．

＊5　定期的なCT/MRI検査として

＊6　動脈的で高吸収域として描出され，静脈相で相対的に低吸収域となるもの．

＊7　胆管細胞癌や転移性肝癌など他の悪性腫瘍が疑われる場合は，各々の精査に進む．

（文献2より）

てもらうための必要な情報として患者心理を配慮しながら説明すべきである．また後述するように肝細胞癌の治療は癌の進行度や背景肝の機能によって治療法が多岐にわたるため，治療法の選択方針が主治医によって多少異なる場合も多い．このため可能な限り初診から同じ医師が患者を担当し治療にあたることも患者との良好な信頼関係を築くうえで重要である．定期的に肝細胞癌のスクリーニング検査をうけ，肝細胞癌の早期発見を医師とともに目指していた患者でも，実際に肝細胞癌が発見されたときの動揺は大きいことを常に念頭においておかなければならない．一方，進行肝細胞癌が発見された場合，患者が

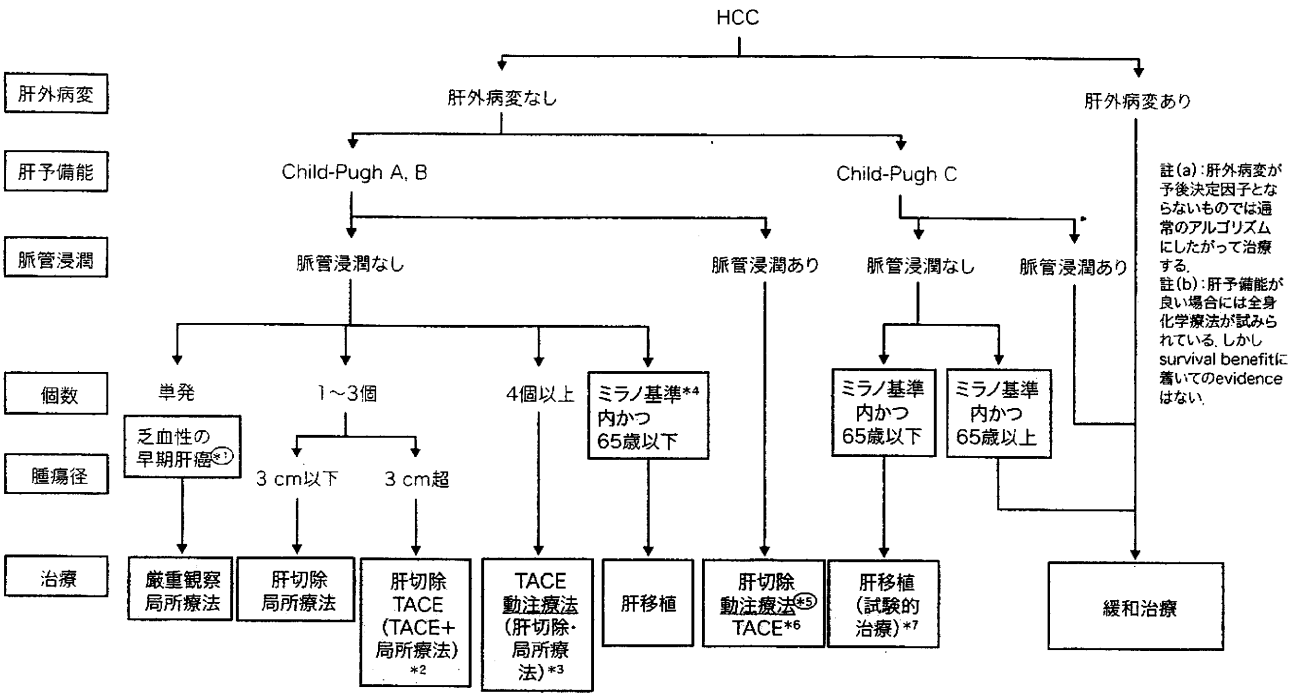

図2　肝細胞癌治療のアルゴリズム(JSHコンセンサス2007)

＊1：乏血性腫瘍は「科学的根拠に基づく肝癌診療ガイドライン」では経過観察が提案されている．しかし，①乏血性で，かつ生検診断で早期肝癌と確診できる病変，または②乏血生でもSPIO-MRI取り込み低下や③CTAPでの血流低下など画像的に悪性所見が確認できる病変は高率に多血生肝癌へ変化することが知れているため，侵襲性の低い局所治療法が行われることが多い．ただし，lead-time bias易除にsurvival benefitがあるか否かのエビデンスはない．

＊2：腫瘍径3 cmを超えるものについてはTACEに加えて局所療法を追加すると局所壊死効果が向上するため，現在の日本ではこの併用療法が行われることが多い．

＊3：可能な場合には肝切除が選択されることがある．また，個数が5～6個以内であればTACEや動注治療を併用して局所治療が追加施行されることも試験的に試みられている．

＊4：ミラノ基準：腫瘍径3 cm以下，腫瘍個数3個以下もしくは単発で5 cm以下．Child-Pugh A/Bでも実際には生体肝移植が選択されるケースもある．

＊5：基本的にリザーバー留置の肝動注化学療法を優先して考える(low dose FP, IFN+5-FUなど)エビデンスは乏しいため，今後，その有効性の検証が必要．

＊6：Vp1, Vp2ではTACEも広く行われている．

＊7：肝移植をしない例では肝性脳症(－)，難治性腹水(－)，Bil＜3.0 mg/dlである場合にはChild-Pugh Cでも局所療法やsubsegmental TAEが選択される場合がある．ただし，survival benefitに関するエビデンスはないので試験的治療として位置づけられる．今後，prospectiveな臨床試験で検証していく必要がある．

(文献3より)

若年者であった場合，他の難治性疾患を合併している場合，あるいは認知症がある場合など，肝細胞癌の告知においても個々の症例に応じた対応が必要な点は他の癌と同様である．

3　肝細胞癌の長期管理

1．細胞癌早期発見のためのスクリーニング

線維化の進行度にもよるがC型慢性肝炎からは年率1～2%，C型肝硬変からは年率6～8%の肝発癌が起こる．したがって癌が出

来てからが長期管理の始まりと捉えるのではなく，発癌前からのスクリーニングも肝細胞癌における長期管理の一部だと考えておくべきである．多くの症例で自覚症状はないため，肝細胞癌高危険群には肝癌のスクリーニング検査として超音波，CTなどの画像検査や腫瘍マーカーの測定を定期的に行う必要がある．具体的には3～6カ月毎の超音波検査とAFP，PIVKA Ⅱの測定を行い，超音波検査や腫瘍マーカーで異常が認められた時には造影CTや造影MRI検査を行う．このような場合にはCTやMRI検査が必要といわれただけでも患者は「遂に癌ができたのではないか」と不安になることが多いので，可能な限り丁寧になぜCTやMRI検査が必要なのかを説明すべきである．現在では図1[2]に示すような肝細胞癌サーベイランスのアルゴリズムが提唱され，施設や担当医の違いに関係なく一定したスクリーニングが可能となってきた．しかし，いくら実際的なアルゴリズムが完成しても患者が検査を受けてくれなければ「絵に描いた餅」ということになる．定期的な肝細胞癌のスクリーニング検査自体は無症状の患者に通院や経済的負担を強いることになり協力を得にくいこともあるが，肝細胞癌の早期発見のための重要な検査であることを患者に理解してもらう必要がある．

2. 肝細胞癌の治療

肝細胞癌が他の癌と異なる点は，肝細胞癌の治療が癌自体の進行度と背景の肝予備能(肝硬変の程度)により決定されることである．図2[3]は日本肝臓学会による肝細胞癌治療のアルゴリズムであるが，肝細胞癌の進展度より上に肝予備能が規定されており，治療を行ううえでいかに肝予備能が重要であるかが示されている．このため最近では肝細胞癌自体の治療と共に，後述するような肝予備能回復のための抗ウイルス療法や栄養療法が積極的に行われている．たとえ小さな肝癌であっても背景肝がChild-Pugh C[4]であれば年齢によっては緩和医療しか行えない場合があることも知っておくべきである．

また，肝細胞癌の治療を行う際には常に治療が肝機能に与える影響を考慮しなければならない．したがって治療に際しては治療後に想定される肝機能や全身状態の変化について事前に説明することは当然であり，さらにその時その時の治療が根治を目指しているのか，あるいは背景肝の機能を考慮した癌のコントロールなのかを説明すべきである．これにより早期に再発を来たしても患者の落胆を軽減できることもあり，次の治療へ円滑に移行することが可能になる．ラジオ波焼灼熱療法から経動脈化学塞栓療法への移行のように前回の治療法と異なる場合に，肝細胞癌の病態が肝予備能も含めてどのように変化したから異なる治療法を選択するのかについても十分な説明を行うべきである．このような治療説明を長年にわたり繰り返すことで患者との信頼関係は強くなり，患者も大きな不安を抱えることなく治療を受けることが可能となる．

3. 肝細胞癌の再発予防

肝細胞癌とくにC型肝炎ウイルス(HCV)感染に起因する肝細胞癌の特徴のひとつは多中心性発癌である．このため早期発見により根治症例が増えてもそののち高率な再発を来たし，このことが肝細胞癌治療による予後改善のための大きなハードルとなっている．最近ではC型肝炎を背景とした肝細胞癌の根治が確認された場合には積極的にインターフェロン治療が行われるようになった．インターフェロンによりHCVが排除された場合には肝線維化が改善することが報告されており，

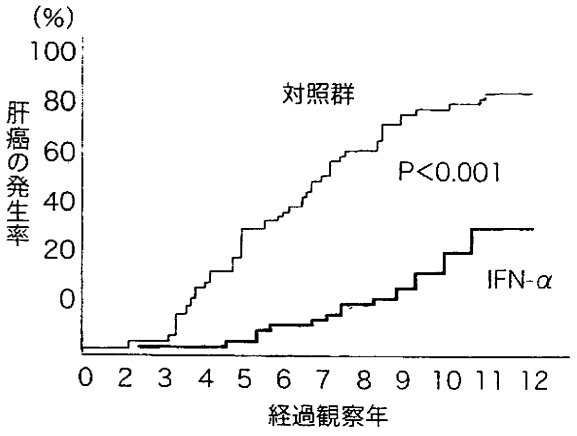

図3　C型肝硬変に対するIFNの発癌抑制効果
（文献5より）

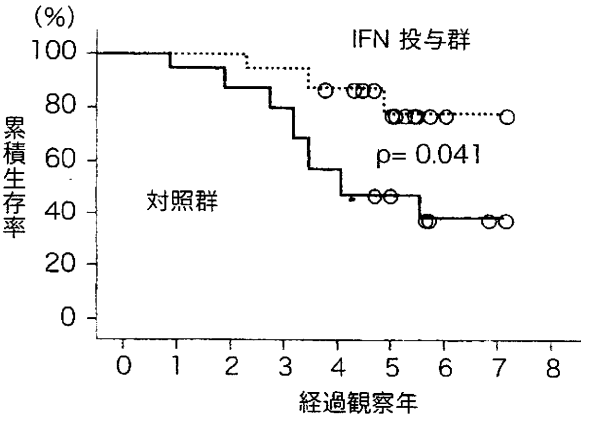

図4　肝癌切除後の累積生存率
（文献6より）

これにより経年的に肝発癌率が低下することも明らかにされている．したがって，肝細胞癌根治後においてもHCVが排除されれば肝細胞癌の再発が抑制されることが予想され，事実本邦からの報告ではインターフェロン治療により肝細胞癌治療後の再発率が抑制されることが示されている（図3，図4）[5-7]．また，Hoshidaらによる外科切除後の肝癌再発抑制を目的としたインターフェロン治療の費用効果の解析では，インターフェロン治療により期待余命は6.1年延長し，生涯医療費が＄77,000増加することにより，増分費用効果は年3％の割引条件で＄15,700と算出され，費用効果の面からもインターフェロン治療の有用性が確認されている[8]．本邦の肝細胞癌患者は年々高齢化しており，この点からも医療経済の問題も無視できない問題である．

一方B型肝炎の肝発癌抑制に関しては，最近Liawらがインターフェロン治療がHBe抗原陽性慢性肝炎患者の肝発癌を抑制することを報告しており（J Hepatol 2007：46；45–52），本邦ではMatsumotoらがB型慢性肝炎における肝発癌抑制にラミブジンが有効であることを報告している（Hepatol Res 2005：32；173–184）．

4．予後改善のための肝硬変に対する栄養療法

肝細胞癌治療を繰り返していくと肝機能は徐々に低下し，肝不全による症状が患者に苦痛を与えることとなる．肝不全を予防するために肝細胞癌のフォローアップ時には常に肝機能の温存に努めることが重要である．肝庇護剤による抗炎症療法や特殊アミノ酸製剤による栄養療法が行われ，肝不全への進行を抑制させる点で成果をあげている．とくに最近では肝硬変自体や肝細胞癌治療に伴う低栄養状態に対して適切な栄養療法を行うことの重要性が指摘されている．

肝硬変では病態の進行に伴いタンパク質，糖，脂質の代謝異常が出現し，約80％の症例で何らかの栄養代謝異常をきたしているとされる．肝硬変ではグリコーゲンの蓄積が減少することで結果的に炭水化物の原料が少ない状態となり，さらにインスリン抵抗性が出現することで糖の利用が困難となり燃料源としての炭水化物の利用率が下がってくる．このためやむなく脂肪を燃焼することになり，非タンパク呼吸商が低下することになる．非タンパク呼吸商は肝硬変患者の生存率を規定する因子のひとつとして報告されている[9]．

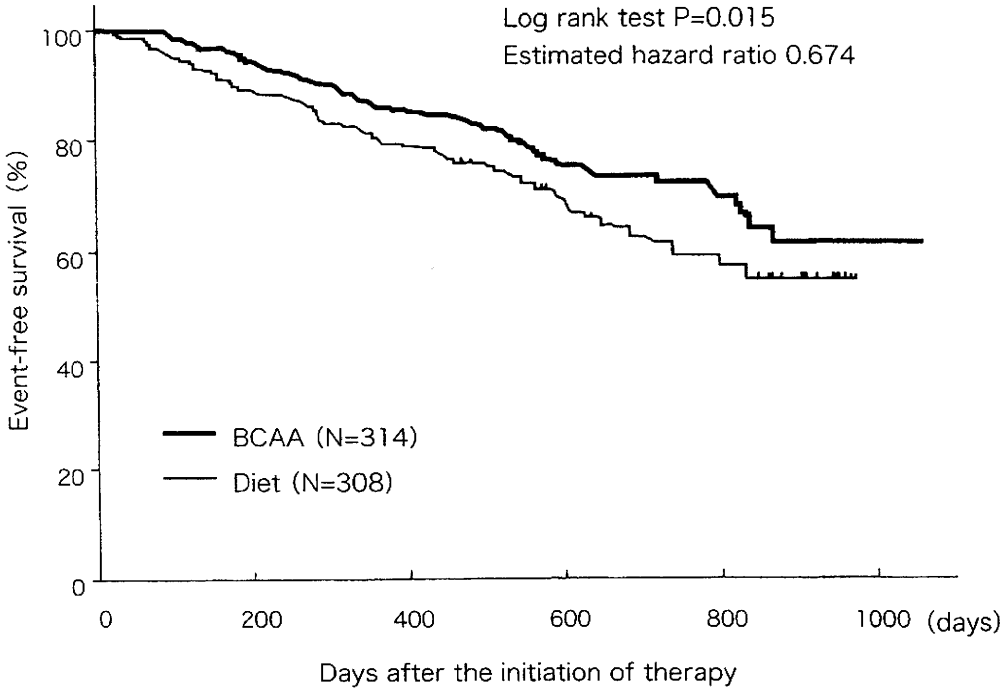

図5　BCAA投与群と食事療法群のイベントフリー生存率の比較(文献11より)

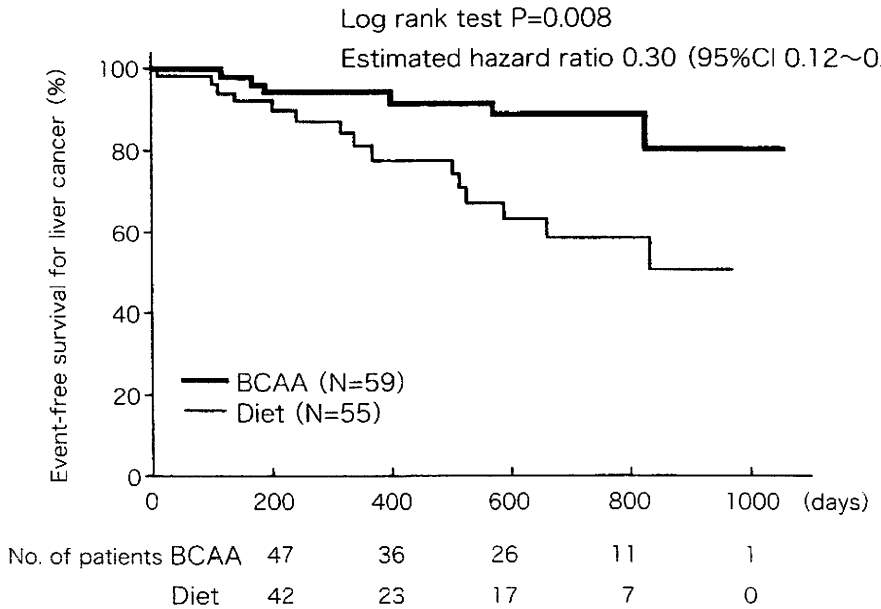

図6　BMI25以上の症例におけるBCAA投与群と食事療法群のイベントフリー生存率の比較(文献8より)

また肝硬変患者ではタンパク合成能が低下しており，血清アルブミン値も非タンパク呼吸商とともに肝硬変患者の独立した予後規定因子であることが確認されている[10]．肝硬変の栄養療法には分岐鎖アミノ酸顆粒や肝不全用経腸栄養製剤が用いられ，有意に肝不全の発症を抑制し，disease-free survival を延長させ(図5)[11]，肝発癌リスクをも低下させることが証明されている(図6，図7)[12]．

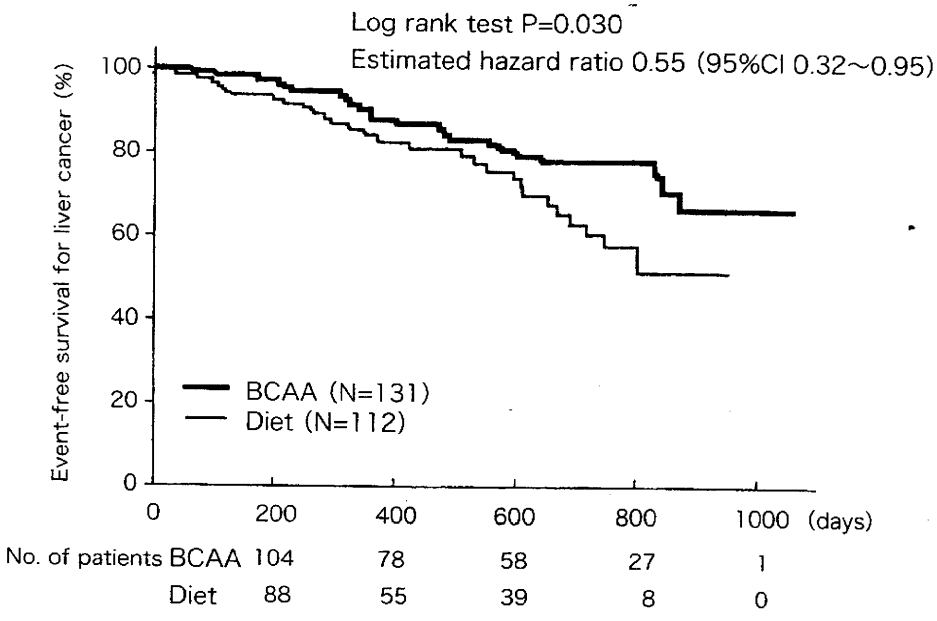

図7　AFP 20 mg/ml以上の症例におけるBCAA投与群と食事療法群のイベントフリー生存率の比較(文献12より)

4 おわりに

本邦の肝細胞癌治は集学的治療という言葉に代表されるように内科的局所療法から外科的切除，あるいは肝移植に至るまで多岐にわたっている．また肝細胞癌のスクリーニングが徹底していることで早期発見されることも多く，治療成績の向上とあいまって肝細胞癌の長期生存例が多く認められるようになった．しかし，その一方で肝内の肝細胞癌のコントロールが可能となることにより，従来とくらべ多臓器転移による症状の出現が増加し，肝細胞患者の長期管理における新たな問題となっている[13]．したがって，病名告知も含め医師が患者とどのように向き合いながら長年にわたる治療を行っていくかは今後ますます重要な課題であり，単に肝細胞癌の治療だけを行えばよいという時代は終わったと考えるべきであろう．

文　献

1) Holland JC, Rowland JH : Handbook of Psychooncology. New York: Oxford Univ Press. 273–282, 1990
2) 科学的根拠に基づく肝癌診療ガイドライン作成に関する研究班編：科学的根拠に基づく肝癌診療ガイドライン2005年度版，金原出版，2005
3) 社会法人日本肝臓学会編：肝癌診療マニュアル，医学書院，2007
4) Pugh RNH, Murray-Lyon IM, Dawson JT et al : Transection of the oesophagus for bleeding oesophageal varices.Br J Surg 60 : 646–649, 1973
5) Yoshida H, Shiratori Y, Moriyama M et al : Interferon therapy reduces the risk for hepatocellular carcinoma: National surveillance program of cirrhostic and noncirrhotic patients with chronic hepatitis C. in Japan. Ann Intern Med 131 : 174–181, 2002
6) Kubo S, Nishiguchi S, Hirohashi K et al : Randomized clinical trial of long-term outcome after resection of hepatitis C virus-related hepatocellular carcinoma by postoperative interferon therapy. Br J Surg 89 : 418–422, 2002
7) Ikeda K, Arase Y, Saitoh S et al : Interferon beta prevents recurrence of hepatocellular carcinoma after complete resection or ablation of the primary tumor-A prospective randomized study of hepatitis C virus-related liver cancer. Hepatology 32 : 228–232, 2000
8) Hoshida Y, Shiratori Y, Omata M : Cost-effectiveness of adjuvant interferon therapy after

surgical resection of hepatitis C-related hepatocellular carcinoma. Liver 22 : 479–485, 2002
9) Tajika M, Kato M, Mohri H et al : Prognostic value of energy metabolism in patients with liver cirrhosis. Nutrition 18 : 229–234, 2002
10) Moriwaki H, Miwa Y, Tajika M et al : Branched-chain amino acids as a protein-and energy-source in liver cirrhosis. Biochem Biophys Res Commun 313 : 405–409, 2004
11) Muto Y, Sato S, Watanabe A et al : Effects of oral branched-chain amino acid granules on event-free survival in patients with liver cirrhosis. Clin Gastroentrol Hepatol 3 : 705–713, 2005
12) 土谷　薫．朝比奈靖浩．泉　並木：分岐鎖アミノ酸（BCAA）長期投与による肝細胞癌再発抑制．日本消化器病学会雑誌 105：808–816．2008
13) Itoh Y, Ohkubo K, Iuchi H et al : Chronological changes of causes of death and distant metastasis in hepatocellular carcinoma. Oncology Reports 9 : 331–335, 2002

*　　*　　*

Liver International ISSN 1478-3223

BASIC STUDIES

Mitochondrial electron transport inhibition in full genomic hepatitis C virus replicon cells is restored by reducing viral replication

Mie Ando[1], Masaaki Korenaga[2], Keisuke Hino[1], Masanori Ikeda[3], Nobuyuki Kato[3], Sohji Nishina[2], Isao Hidaka[2] and Isao Sakaida[2]

1 Department of Basic Laboratory Sciences, Yamaguchi University Graduate School of Medicine, Yamaguchi, Japan
2 Department of Gastroenterology and Hepatology, Yamaguchi University Graduate School of Medicine, Yamaguchi, Japan
3 Department of Molecular Biology, Okayama University Graduate School of Medicine, Dentistry, and Pharmaceutical Sciences, Okayama, Japan

Keywords
fluvastatin – interferon – oxidative stress – reactive oxygen species

Correspondence
Keisuke Hino, MD, PhD, Department of Hepatology and Pancreatology, Kawasaki Medical University, 577 Matsushima Kurashiki, Okayama 701-0192, Japan
Tel: +81 86 4621111
Fax: +81 86 4641196
e-mail: khino@med.kawasaki-m.ac.jp

Received 25 September 2007
Accepted 30 January 2008

DOI:10.1111/j.1478-3231.2008.01720.x

Abstract

Background/Aim: Hepatitis C virus (HCV) core protein has been shown to inhibit mitochondrial electron transport and to increase reactive oxygen species (ROS) *in vitro* and *in vivo*. The aim of this study was to investigate whether inhibiting HCV replication could restore the mitochondrial redox state and electron transport activity. *Methods:* We measured ROS, mitochondrial reduced glutathione content, and mitochondrial complex I, II, III and IV activities and protein expression in full genomic HCV replicon cells and cured cells that had been prepared by eliminating HCV RNA from replicon cells by interferon (IFN)-α treatment. *Results:* Cured cells had significantly lower ROS production and greater mitochondrial glutathione content than replicon cells. Complete inhibition of HCV replication by IFN-α restored complex I and IV activities by 20–30% ($P < 0.01$) and complex I expression ($P < 0.05$). Treatment with fluvastatin, one of the 3-hydroxy-3-methylglutaryl co-enzyme A reductase inhibitors, which is known to have anti-HCV activity, partially inhibited core protein expression and restored complex I activity in full genomic HCV replicon cells to a lesser degree ($P < 0.05$). *Conclusions:* Our results show that the mitochondrial redox state and electron transport activity can be restored by reducing HCV replication.

Hepatitis C virus (HCV) causes acute and chronic hepatitis, cirrhosis and hepatocellular carcinoma (HCC) (1). Because current antiviral treatment can only eliminate the virus in about 50% of patients (2, 3), therapies to reduce disease progression in chronically infected individuals would be of great benefit. In this respect, it is still a matter of debate whether reduction of HCV replication, even if not eliminating HCV, is beneficial to the outcome of disease. Although the mechanisms of its pathogenesis are incompletely understood, there have been several lines of evidence suggesting that oxidative stress is present in chronic hepatitis C to a greater degree than in other inflammatory liver diseases and is closely related to disease progression (4, 5). We and others have shown that HCV core protein induces the production of reactive oxygen species (ROS) (6–8) and that mitochondrial electron transport inhibition by HCV is associated with ROS production (9). Therefore, whether reduction of HCV replication restores mitochondrial electron transport activity is of interest in exploring treatments to reduce disease progression in HCV-associated chronic liver disease.

Establishment of the HCV subgenomic replicon has made it possible to assess the antiviral activities of interferon (IFN) and other reagents *in vitro* (10). We also developed a genome-length HCV RNA replication reporter system (11) and found that different statins, which are 3-hydroxy-3-methylglutaryl co-enzyme A reductase inhibitors, have different anti-HCV profiles while using this reporter system (12). In the present study, we chose to use fluvastatin, which exhibited the strongest inhibition of HCV replication among the statins (12), to reduce HCV replication in full genomic HCV replicon cells without complete inhibition. The aim of this study was to examine whether mitochondrial electron transport activity was restored by reduction of HCV replication.

Materials and methods

Cell cultures

Full genomic HCV replicon cells were described in detail by Ikeda *et al.* (11). Cells were cultured in Dulbecco's modified Eagle's medium supplemented with 10% fetal calf serum, penicillin, streptomycin and G418 (300 μg/ml; Calbiochem, Darmstadt, Germany) and passaged twice a week at a 5:1 split ratio. Cured cells were established by eliminating genome-length HCV RNA from replicon cells by IFN-α treatment (500 IU/ml for 2 weeks; Sigma-Aldrich, St Louis, MO, USA) without G418, as described (11). In some experiments, full genomic HCV replicon cells were incubated in the presence of 10 μmol/L fluvastatin (Novartis Pharmaceutical, Tokyo, Japan) for 96 h.

Measurement of reactive oxygen species

The cellular ROS level was measured by oxidation of the cell-permeable, oxidation-sensitive fluorogenic precursor dihydrodichlorocarboxyfluorescein diacetate (DCFDA; Molecular Probes Inc., Eugene, OR, USA). Cells in six-well plates were treated with tertiary butyl hydroperoxide (t-BOOH) for 5 h or not, followed by a 30-min incubation with DCFDA (500 nmol/L final concentration) at 37 °C. Fluorescence was measured with a CytoFluorII fluorescence plate reader (PerSeptive Biosystems, Framingham, MA, USA) at an excitation wavelength of 486 nm and an emission wavelength of 530 nm as described (7).

Localization of ROS production on the subcellular level was observed with a Zeiss (Oberkochen, Germany) LSM5 Pascal inverted laser scanning confocal microscope. Cells were pre-incubated with 5 μmol of hydroxyphenyl florescein (HPF, Alexis Corporation, Lausen, Switzerland) (13) for 5 min at 37 °C. They were then imaged at 30-s intervals after treatment with 10 nmol/L t-BOOH. The green fluorescence of HPF (excitation, 488 nm; emission, 505–530 nm) was observed after excitation with an argon–krypton laser.

Isolation of mitochondria

Mitochondrial pellets were obtained as described previously with some modification (7, 9). Briefly, harvested cells were centrifuged at 500*g* for 5 min. The pellets were homogenized with 25 strokes using a Dounce homogenizer (Wheaton Science Products, Millville, NJ, USA) and a tight-fitting pestle with isolation buffer [70 mM sucrose, 1 mM KH_2PO_4, 5 mM HEPES, 220 mM mannitol, 5 mM sodium succinate and 0.1% bovine serum albumin (BSA), pH 7.4]. The homogenate was centrifuged at 1330*g* for 5 min at 4 °C. The supernatant fraction was retained, whereas the pellet was washed with isolation buffer and centrifuged again. The combined supernatant fractions were centrifuged at 1000*g* for 15 min at 4 °C to obtain a crude mitochondrial pellet. Purified mitochondria were prepared by sucrose gradient (1.5 M sucrose and 1 M sucrose) centrifugation as described (14) with some modification. An aliquot was removed for determination of the protein concentration with the Bio-Rad protein DC assay kit (Bio-Rad, Hercules, CA, USA), using BSA as the standard.

Measurement of reduced glutathione content

Crude mitochondrial samples (3–4 mg of mitochondrial protein) were sonicated using a Sonifier cell disruptor 200 (VWR Scientific, Danbury, CT, USA) for 15 s at power setting 3 in ice-cold 5% metaphosphoric acid and centrifuged at 3000*g* at 4 °C for 10 min. The concentration of reduced glutathione was measured by the thioester method using a GSH-400 kit (Oxis International Inc., Portland, OR, USA).

Immunoblotting

Crude mitochondrial pellets were suspended in lysis buffer (T-PER Tissue Extraction Reagent; Pierce, Rockford, IL, USA) and centrifuged at 10 000*g* for 15 min at 4 °C. The supernatant (20 μg of protein) was separated by sodium dodecyl sulphate-polyacrylamide gel electrophoresis on 16% gel. The proteins were electrophoretically blotted onto polyvinylidene difluoride membranes (Millipore, Bedford, MA, USA), blocked overnight at 4 °C with 5% skim milk and 0.1% Tween 20 in Tris-buffered saline, and subsequently incubated for 1 h at room temperature with an anti-hepatitis C core protein antibody (1:1000, Affinity Bio Reagents, Golden, CO, USA), anti-OxPhos complex I antibody (1:1000), anti-OxPhos complex II antibody (1:2000), anti-OxPhos complex III antibody (1:2500) or anti-OxPhos complex IV antibody (1:1000, Molecular Probes Inc). The membranes were washed, incubated with appropriate secondary antibodies and detected with ECL™ Western blot detection reagents (Amersham Biosciences, Piscataway, NJ, USA). The degree of protein expression was expressed as the normalized quotient, which was derived by dividing the intensity of the blot density of each protein by that of β-actin protein.

Measurement of complex I, II, III and IV activities

Submitochondrial particles were prepared from mitochondria by incubation for 3 min at 37 °C followed by sonication in a microcentrifuge tube immersed in ice water. Forty micrograms of submitochondrial

particles was pelleted at 15 000*g* for 10 min. Enzyme activity assays were performed at 25 °C by a previously established method (15). Complex I [nicotinamide adenine dinucleotide (NADH)-decylubiquinone oxidoreductase] activity was measured as the initial (5 min) rate of decrease of A_{340} using the acceptor 2,3-dimethoxy-5-methyl-6-*n*-decyl-1,4-benzoquinone (DB 80 μM) and 200 μM NADH as the donor in 10 mM Tris (pH 8.0) buffer containing 1 mg/ml BSA, 0.24 mM KCN and 0.4 μM antimycin A. Complex II (succinate decylubiquinone 2,6-dichlorophenolindophenol reductase) activity was measured at 600 nm using 80 μM DCPIP as the acceptor and 10 mM succinate as the donor in 10 mM KH_2PO_4 (pH 7.8), 1 mg/ml BSA, 2 mM EDTA, in the presence of 0.24 mM KCN, 4 μM rotenone, 0.2 mM ATP and 0.4 μM antimycin A. Complex III (ubiquinol cytochrome *c* reductase) activity was measured at 550 nm using 40 μM oxidized cytochrome *c* as the acceptor and 80 μM decylubiquinol as the donor in 10 mM KH_2PO_4 (pH 7.8), 1 mg/ml BSA, 2 mM EDTA, in the presence of 0.24 mM KCN, 4 μM rotenone and 0.2 mM ATP for 2 min. Complex IV (cytochrome *c* oxidase) activity was measured using a cytochrome *c* oxidase assay kit (Sigma-Aldrich), following the manufacturer's instructions.

Statistical analysis

Quantitative values are expressed as mean ± standard deviation. Two groups were compared by the Student *t*-test. A P value of < 0.05 was considered to be significant. Two groups among multiple groups were compared by the rank-based, Kruskal–Wallis analysis of variance test followed by Scheffe's test.

Results

Increased reactive oxygen species production and mitochondrial oxidant status in full genomic hepatitis C virus replicon cells

To assess the effect of HCV replication on ROS production, we used the ROS-sensitive fluorescent probe DCFDA. As compared with cured cells, HCV replication increased ROS 1.4-fold (Fig. 1A). Because HCV infection results in an inflammatory response and an increase in the basal oxidative stress, we next determined the effect of an exogenous oxidant, 500 nmol/L t-BOOH, on ROS production. This treatment had no effect on cured cells, but increased ROS production in full genomic HCV replicon cells to a level 2.5-fold greater than that of cured cells (Fig. 1A; $P < 0.01$). Cells were then imaged by confocal microscopy at 30-s intervals after exposure to HPF, which is more sensitive to ROS production than DCFDA. As shown in Figure 1B, treatment with t-BOOH significantly increased the oxidized fluorescent product as time passed in full genomic HCV replicon cells, but not in cured cells ($P < 0.0005$). Thus, a small volume of exogenous oxidant (10 nmol/L) that did not induce ROS production in cured cells significantly increased ROS production in full genomic HCV replicon cells.

We previously demonstrated, by confocal microscopy, that the mitochondria are the primary site of initial ROS production in cells expressing HCV core protein and cytochrome P450 2E1 (7). Because confocal microscopic images of the oxidized fluorescent product in replicon cells were almost the same as those in our previous study, we measured mitochondrial reduced glutathione content to assess mitochondrial antioxidant capacity. The level of mitochondrial reduced glutathione was significantly lower in full genomic HCV replicon cells than in cured cells (Fig. 1C; $P < 0.05$), suggesting that HCV replication was responsible for the mitochondrial oxidant status and sensitized to exogenous oxidative stress.

Restoration of mitochondrial electron transport activity by complete inhibition of hepatitis C virus replication

Our previous study has demonstrated that core protein causes oxidation of the glutathione pool, increases ROS production and inhibits complex I activity (9). Because increased ROS production and mitochondrial oxidant status were found in full genomic HCV replicon cells as well, we next measured complex I, II, III and IV activities in submitochondrial particles to determine whether inhibiting HCV replication restored mitochondrial electron transport activity. Complete inhibition of HCV replication by IFN-α restored complex I and IV activities by 20–30% ($P < 0.01$) (Fig. 2). However, complex II and III activities were not changed after treatment with IFN-α in these cells (Fig. 2).

We further assessed the expression levels of complexes I, II, III and IV in full genomic HCV replicon cells and cured cells. As shown in Figure 3, immunoblotting revealed that complete inhibition of HCV replication by IFN-α restored the complex I expression as well ($P < 0.05$). Although the complex IV activity was restored by IFN-α, the expression of complex IV did not change after complete inhibition of HCV replication. Thus, it should be noted that both activity and expression of complex I were restored by completely inhibiting HCV replication in full genomic HCV